Mutational Analysis of a Sequence-Specific ssDNA Binding Lupus Autoantibody†

Joanne Cleary and Gary D. Glick*

Departments of Chemistry and Biological Chemistry, University of Michigan, Ann Arbor, Michigan 48109-1055

Received May 31, 2002; Revised Manuscript Received September 23, 2002

ABSTRACT: 11F8 is a murine anti-ssDNA monoclonal autoantibody isolated from a lupus prone autoimmune mouse. This mAb binds sequence specifically, and prior studies have defined the thermodynamic and kinetic basis for sequence-specific recognition of ssDNA (Ackroyd, P. C., et al. (2001) *Biochemistry 40*, 2911−2922; Beckingham, J. A. and Glick, G. D. (2001) *Bioorg. Med. Chem. 9*, 2243−2252). Here we present experiments designed to identify the residues on 11F8 that mediate sequence-specific, noncognate, and nonspecific recognition of ssDNA and their contribution to the overall binding thermodynamics. Site-directed mutagenesis of an 11F8 single-chain construct reveals that six residues within the complementarity determining regions of 11F8 account for ca. 80% of the binding free energy and that there is little cooperativity between these residues. Germline-encoded aromatic and hydrophobic side chains provides the basis for nonspecific recognition of single-stranded thymine nucleobases. Sequence-specific recognition is controlled by a tyrosine in the heavy chain along with a somatically mutated arginine residue. Our data show that the manner in which 11F8 achieves sequence-specific recognition more closely resembles RNA-binding proteins such as U1A than other types of nucleic acid binding proteins. In addition, comparing the primary sequence of 11F8 with clonally related antibodies that differ by less than five amino acids suggests that somatic mutations which confer sequence specificity may be a feature that distinguishes glomerulotrophic pathogenic anti-DNA from those that are benign.

Defining the structural and thermodynamic basis of protein·nucleic acid recognition is of fundamental importance for developing a better understanding of cellular regulation. Antibodies that bind nucleic acids provide a unique model system to characterize nucleic acid-binding proteins. All antibodies possess a conserved structural framework; antigen specificity is defined by small variations within the complementarity determining regions (CDRs)[1] in the binding site (*1*). Therefore, antibodies can be used to study how defined changes in sequence can affect ligand recognition. Antibodies that bind DNA (anti-DNA) are also of interest from a clinical perspective, as they are a prominent serological hallmark of the autoimmune disorder systemic lupus erythematosus (SLE) (*2*). Moreover, a subset of anti-DNAs are also pathogenic: they bind DNA adherent to the glomerular basement membrane in the kidney and incite an inflammatory response (known as lupus nephritis or glomerulonephritis) resulting in renal damage (*3*). At present, however, there is no basis a priori to differentiate pathogenic anti-DNA from those that are benign (*2*, *4*, *5*).

The in vitro binding properties of monoclonal anti-DNA have been extensively investigated (*6*−*9*). These studies have started to reveal such features as the structure of anti-DNA (*10*, *11*, *12*), their complexes with DNA ligands (*13*, *14*), and the kinetics (*15*) and thermodynamics (*16*−*19*) of DNA binding. In experiments using synthetic DNA homo/heteropolymers and high molecular weight nucleic acids as test antigens (e.g., plasmids or genomic DNA), it has been determined that anti-DNA recognize either ssDNA, dsDNA, or cross-react between both forms of DNA (*2*, *6*, *20*). In addition, experiments have demonstrated that anti-dsDNA can possess considerable binding specificity (*18*, *21*). For example, Herrmann et al. have found that human SLE sera enriched for anti-dsDNA preferentially bind certain duplex sequences, possibly in a sequence specific fashion (*22*). In addition, several laboratories have found that lupus anti-ssDNA are often base specific, recognizing one homopolymer in preference to others (typically polyT) (*2*, *6*, *17*, *19*, *23*). From both a structural and thermodynamic perspective, some aspects of this binding are similar to that seen for other ssDNA-binding proteins such as the phage T4 gene 32 protein and the phage M13 gene 5 protein (*24*−*28*).

In previous experiments, we generated a panel of anti-ssDNA monoclonal autoantibodies (mAb) from an autoimmune MRL/*lpr* mouse (*29*). One mAb from this panel, 11F8, is pathogenic; it localizes to kidney tissue by binding to DNA adherent to the glomerular basement membrane (*30*). Using binding-site selection experiments in combination with affinity and footprinting measurements, we provided evidence that 11F8 is sequence specific (*31*) using accepted criteria to assess sequence specificity (*32*). Sequence-specific recognition by 11F8 is achieved when functional groups on its high affinity consensus sequence (**1**) are presented within a well-defined secondary structure (Figure 1). Single-stranded residues *10*−*12* on **1** provide critical sequence-dependent

† Supported by NIH Grant GM 46831.

* Corresponding author. Phone: (734) 764-4548. FAX: (734) 763-2307. E-mail: gglick@umich.edu.

[1] Abbreviations: anti-DNA autoantibodies, anti-DNA; complementarity determining region, CDR; dimethyl sulfate, DMS; double-stranded DNA, dsDNA; *Esherichia coli*, *E. coli*; monoclonal antibodies, mAbs; potassium permanganate, $KMnO_4$; single-stranded DNA, ssDNA; systemic lupus erythematosus, SLE; V_H, variable heavy; V_L, variable light. $^aX^b$: a represents the germline-encoded amino acid, X denotes the CDR, and b represents the somatic mutation.

10.1021/bi0203942 CCC: $25.00
Published on Web 12/10/2002

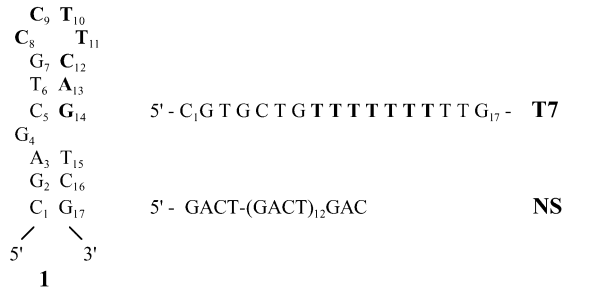

FIGURE 1: DNA ligands used in binding studies. Binding site selection experiments were conducted with 11F8 and 55-nucleotide-long ssDNA constructs possessing a seven-nucleotide-long random insert (*31*). DNA of known sequence designed to prevent formation of stable secondary structure flanked the random region. **1** is the consensus sequence obtained from these experiments (*31*). Additional nucleotides flanking the stem-loop are not shown (represented as ~) and are part of the PCR primers used in the selections. Mutations produced during PCR amplification at multiple sites within the constant region afforded a stable secondary structure that was selected for by 11F8. In **T7**, positions 3, 8−14, and 16 of **1** are replaced with T.

recognition contacts, whereas the bases in the stem duplex, including the bulge, serve only to preorganize the recognition elements of **1** (due to fraying at the stem-loop junction, dC_{12} possesses single-strand character, as evidenced by NMR, and its reactivity to single-strand specific footprinting reagents; *16*, *31*). Binding of **1** is enthalpy-driven, opposed by entropy, and accompanied by a negative change in heat capacity. The thermodynamic driving force for sequence-specific recognition is the release of incompletely hydrogen bonded water molecules from the hydrophobic binding site, concomitant with the formation of two salt bridges (*15*, *16*).

Here we present the results of site-directed mutagenesis experiments designed to elucidate the role of basic and hydrophobic residues in sequence-specific, noncognate, and nonspecific binding. Because the sequence and structure of **1** are closely related to DNA antigens present in human anti-DNA·DNA complexes (*33*) and 11F8 is glomerulotrophic (*30*), this system provides an anti-DNA mAb·DNA model relevant to human lupus. Characterization of this system could therefore provide insight to advance diagnosis (e.g., a basis to differentiate pathogenic anti-DNA from those that are benign) and treatment (e.g., a means to interfere with anti-DNA·DNA interactions) of lupus. Moreover, while a number of sequence-specific ssDNA binding proteins have been reported (e.g., *34*, *35*), comparatively less is known about the structural and thermodynamic basis for sequence discrimination relative to dsDNA and RNA binding proteins. From a more fundamental standpoint, therefore, 11F8 represents a unique model to probe mechanistic aspects of sequence-specific ssDNA interactions.

MATERIALS AND METHODS

Plasmids, Bacterial Strains, and Media. The pET-28b-(+) vector (Novagen, Madison WI) was used for cloning and expression. *Escherichia coli* (*E. coli*) strain DH5α was the host for manipulation of plasmids, and BL21(DE3) strain was used for T7 polymerase-driven gene expression (*36*). In all procedures, LB medium was used, and kanamycin (30 μg/mL) (Boehringer Mannheim, Indianapolis, IN) was added for growth and expression in both DH5α and BL21(DE3) strains.

Construction, Cloning, and Expression of sc11F8. Construction of sc11F8 was performed by overlap extension PCR (*37*) of V_L and V_H cDNA with the 14-amino acid linker (202: EGKSSGSGSESKST) with restriction enzyme sites incorporated at the 5′ and 3′ ends (*Nco*I and *Not*I, respectively) for ligation into pET-28b(+). Oligonucleotides used in PCR reactions were synthesized by the solid-phase phosphoramidite method, on a Millipore Expedite 8909 DNA/RNA synthesizer using standard protocols as previously described (*29*).

Following amplification by PCR, the single-chain product (*Nco*I-V_L-202-V_H-*Not*I) was purified by electrophoresis in agarose gel (1.5%) and recovered with QIAGEN GelExtraction Kit (QIAGEN Inc., Santa Clarita, CA). After digestion with the restriction enzymes *Nco*I and *Not*I (New England Biolabs Inc., Beverly, MA), the single-chain was ligated into *Nco*I/*Not*I cut pET-28b(+) vector (Novagen, Madison, WI). The construct was ligated in-frame with the C-terminal $(His)_6$ sequence present in the vector to allow for protein identification and purification. Correct clones were identified by restriction analysis followed by small scale protein expression in *E. coli* strain BL21(DE3).

Large-Scale Expression and Isolation of sc11F8. For large scale expression of sc11F8, an overnight culture in LB (10 mL) containing kanamycin was used to innoculate 1 L of media. Cells were grown at 37 °C until $OD_{600} = 0.6$, at which point protein expression was induced by addition of isopropyl β-D-thiogalactopyranoside (IPTG) (to 1 mM final concentration). After 3 h at 37 °C, cells were centrifuged for 15 min at 6000*g* at 4 °C.

Isolation of sc11F8 from the insoluble bacterial pellet was performed by addition of lysis buffer (50 mM Tris, pH 8, 1 mM EDTA, 200 μg/mL lysozyme, 0.1 mM phenylmethanesulfonyl fluoride; 2 mL per L of cell culture), followed by sonication (3 × 10 s). After centrifugation for 30 min at 20 000*g*, cell pellets were resuspended in lysis buffer (1.5 mL per L culture), sonicated, and centrifuged for 30 min at 20 000*g*. Cells were then resuspended in lysis buffer (1.5 mL per L of culture) containing Triton X-100 (0.5%), centrifuged for 15 min at 20 000*g*. The last step was then repeated without Triton X-100. The pellet was solubilized in guanidine−HCl (6 M) in Ni^{2+} column binding buffer (50 mM K_2HPO_4 pH 8, 300 mM NaCl; 2 mL per L of culture), sonicated (3 × 10 s), placed on ice for 1 h, and then centrifuged for 45 min at 25 000*g*. The supernatant was decanted, diluted 1:1 with Ni^{2+} column binding buffer, and filtered through a 0.45 μM syringe filter (Millipore, Bedford, MA).

The supernatant was added to Ni^{2+} resin (1.0 mL) (QIAGEN Inc., Santa Clarita, CA) that was preequilibrated with guanidine−HCl (6 M) in Ni^{2+} column binding buffer. The resin was then washed with 10 column volumes of binding buffer containing guanidine−HCl (6 M) and imidazole (5 mM) and then with 10 column volumes of binding buffer containing guanidine−HCl (6 M) and imidazole (20 mM). The sc11F8 protein was eluted from the column with binding buffer containing guanidine−HCl (6 M) and imidazole (250 mM). The protein was refolded by rapid dilution (1:200) into DNA binding buffer (50 mM K_2HPO_4, pH 8, 150 mM NaCl) for 36 h at 4 °C.

The sc11F8 protein was concentrated (to ca. 10 mL) using an Amicon Ultrafiltration stirred pressure cell (YM10

membrane; Millipore, Bedford, MA), and added to single-stranded DNA agarose matrix (1 mL) (Gibco, Rockville, MD). The resin was washed with five column volumes of DNA binding buffer, and the protein was eluted from the column with DNA binding buffer containing NaCl (2 M) and immediately exchanged into 50 mM K_2HPO_4 pH 8.0, 150 mM NaCl by dialysis. Protein purified with this procedure was >98% pure on the basis of SDS−PAGE analysis.

Construction of sc11F8 Mutants. The sc11F8 (*Nco*I−V_L−202-V_H−*Not*I) in pET-28b(+) was used as the template for mutagenesis. PCR methodology was used to incorporate a single amino acid substitution into the wild-type sequence using the "megaprimer" method (*38*). Following amplification, mutant PCR products were purified, ligated, and transformed as described for the wild-type construct. Successful incorporation of the mutation was confirmed by DNA sequencing. Large-scale expression and purification were performed as described for the wild-type protein.

Guanidine−HCl Unfolding of Wild-Type sc11F8 and Mutants. Protein samples were equilibrated for 1 h at 25 °C in denaturing buffer (20 mM Tris, 150 mM NaCl, pH 8.0) with guanidine−HCl (Pierce, Rockford, IL) ranging from 0.1 to 6 M. The intrinsic tyrosine and tryptophan protein fluorescence (λ_{ex} = 280 nm; λ_{emm} = 338 nm; 16 nm emission band-pass) was then measured as a function of guanidine−HCl concentration. Each value was corrected for the background fluorescence signal at each concentration of guanidine−HCl. The fraction of unfolded protein was calculated as previously described (*39*). The free energy of unfolding in the absence of guanidine−HCl and concentration of guanidine at which half the protein is unfolded, C_m, were determined by assuming a linear extrapolation model (*39*).

Steady-State Fluorescence Affinity Measurements. Fluorescence measurements were carried out on a Spectronic AB2 fluorimeter equipped with a magnetic stirrer and thermostat cellblock as previously described (*16*). In short, sc11F8 was diluted into titration buffer (20 mM Tris, variable [MX], temperature, and polarity) and allowed to equilibrate at the desired temperature. The intrinsic protein fluorescence (λ_{emm} 338 nm; 16 nm emission band-pass) was measured as a function of added DNA. In general, titrations for wild-type sc11F8 and tight binding protein mutants used 280 nm excitation wavelength, while weakly binding protein mutants used 285 or 290 nm excitation wavelength. Dissociation constants were obtained from fluorescence intensity values as previously described (*16*).

van't Hoff Experiments. Binding titrations were carried out over the temperature range 5 to 35 °C (20 mM Tris; 150 mM NaCl, pH 8). To correct for pH variation of the buffer with temperature, separate buffers were made at the appropriate titration temperature. Data were plotted in van't Hoff form (log K_{obs} vs 1/T) and analyzed using the KaleidaGraph software. Enthalpy values were calculated using either the linear van't Hoff equation or a series of relationships that assume constant heat capacity change, as previously described (*16*, *40*, *41*).

Salt Studies. Binding titrations were carried out over [NaCl] concentration range of 85−400 mM and [NaOAc] range of 100−500 mM. The slope of the plot (−log[K_{obs}] vs log[MX]) represents the stoichiometry of salt release (*42*). Salt release stiochiometry values in NaOAc were interpreted in terms of number of ionic interactions present in the complex, as previously described (*16*, *42*, *43*). The overall binding energy provided by ion release was estimated using eq 1 (*44*):

$$\Delta G_{\text{ion release}} = -(\mathbf{a} + \mathbf{c})\, RT \ln [\text{MX}] \qquad (1)$$

where the coefficient (**a** + **c**) represents the stiochiometry of ion release.

Osmotic Stress and Polarity Experiments. For the polarity and osmotic stress experiments, fluorescence titrations were conducted in buffer containing 4−20% (w/v) methanol, ethanol, and 1-propanol (Sigma, St. Louis, MO). Osmolal concentrations were calculated from the solute weight percent using published tables (*45*).

Footprinting sc11F8 and Mutant·DNA Complexes. 11F8 and 5′ ^{32}P end-labeled DNA were incubated in buffer (10 mM Tris, 150 mM NaCl, pH 8) containing dA_{21} as a nonspecific competitor (1 μM). In these experiments, excess protein was used to ensure that all DNA was bound. Potassium permanganate ($KMnO_4$) or dimethyl sulfate (DMS) footprinting was then performed and the data analyzed as previously described (*29*, *46*).

RESULTS

Selection of Mutants. The goals of this study were to identify the residues on 11F8 that mediate sequence-specific, noncognate, and nonspecific recognition of ssDNA and the contribution of these residues to the overall binding thermodynamics. Mutagenesis experiments initially focused on the V_H of 11F8 since residues within the heavy chain CDRs of anti-DNA antibodies are generally more important to antigen binding than those in the V_L(*17*, *47*−*49*). To avoid introducing gross structural changes into the ssDNA antigen binding site, residues that maintain the canonical structure of the CDRs (excluding HCDR3) or that participate in CDR−CDR interactions were not chosen for mutagenesis (*50*). Analysis of the 11F8 germline gene sequence reveal two somatic mutations, ^{V9}FW1^{A} and ^{S31}HCDR1$^{R(1)}$ (*51*, *52*). The valine to alanine mutation is a conservative change in the framework region and is not expected to effect antigen recognition (*1*). However, because S31R is in a hypervariable region, this mutation may alter the affinity and/or specificity for DNA and was chosen for analysis.

Sequence-specific binding of **1** by 11F8 is driven by hydrophobic interactions between nonpolar protein side chains and ssDNA surfaces, with accompanying desolvation of nonclathrate water structures (*16*). Because L97 in HCDR3 is the most hydrophobic residue in the V_H CDRs of 11F8, it was selected for study. Sequence analysis of 11F8 reveals several tyrosine residues in the CDRs at sites previously implicated in DNA recognition: Y32 in LCDR1, Y32 in HCDR1, Y56 in HCDR2, as well as Y99 and Y100 in HCDR3 (*13*, *53*−*55*). As such, these residues were also chosen for mutagenesis. In addition, binding of DNA by 11F8 quenches the intrinsic fluorescence at excitation wavelengths of 295 nm, which suggests that tryptophan residues are involved in recognition (*56*, *57*). Although there are five tryptophan residues in 11F8, only ^{W33}HCDR1 is located within the CDRs. Hence, it is possible that this residue participates directly in binding and was also chosen for mutagenesis.

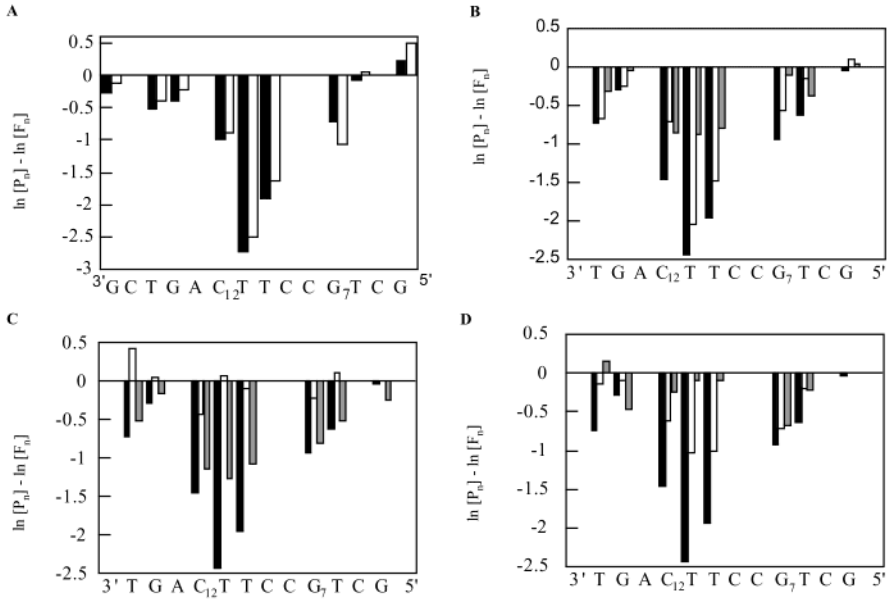

FIGURE 2: Quantification of $KMnO_4$ and DMS protection footprinting. (A) sc11F8·**1** (black bars) and F(ab)·**1** (white bars); (B) sc11F8·**1** (black bars), R31K·**1** (white bars), and R31Q·**1** (gray bars); (C) sc11F8·**1** (black bars), $Y32_LA$·**1** (white bars), and W33V·**1** (gray bars); (D) sc11F8·**1** (black bars), L97A·**1** (white bars), and Y100V·**1** (gray bars). The data were analyzed as previously described (*16*). The difference in strand cleavage is represented by bars and is calculated by subtracting the logarithm of the probability of cleavage at each position in the free DNA (F_n) from the same position in the complex (P_n) (*46*). A larger negative value of $\ln(P_n/F_n)$ indicates greater protection from $KMnO_4$ or DMS modification.

Upon binding to 11F8, cations are released from the phosphate backbone of ssDNA ligands. Cation release generally results from salt bridge formation between positively charged residues and the DNA backbone and may be interpreted in terms of number of ionic interactions present in the complex (*42*, *58*). In addition to R31 discussed above, there are four other basic residues in the V_H CDRs: ^{K62}HCDR2, ^{K64}HCDR2, ^{R96}HCDR3, and ^{R98}HCDR3. Previous studies of anti-DNA have emphasized the importance of arginine versus lysine in DNA recognition (*48*, *59*−*62*). Thus, R96 and R98 were chosen for study.

Characterization of sc11F8. The V_H and V_L regions of 11F8 were cloned and expressed in *E. coli* as a single-chain construct (designated sc11F8). The single-chain protein was constructed by joining the C-terminus of V_L to the N-terminus of V_H using a 14 amino acid flexible linker, designated "202" (EGKSSGSGSESKST) (*63*). However, single chain constructs do not necessarily retain the same binding characteristics as the corresponding Ig or F(ab) fragments (*63*−*65*). To confirm that sc11F8 retains the same binding properties as the parent F(ab), footprinting experiments and affinity measurements as a function of various solution conditions were conducted (*16*). Collectively, these data demonstrate that the affinity, specificity, and thermodynamics of binding by sc11F8 is indistinguishable from 11F8 F(ab) (Figure 2A, Table 1).

Relative Affinity of Mutant Proteins: *Arginine Residues*. To investigate the role of arginine in DNA binding by 11F8, residues R31, R96, and R98 of 11F8 were each mutated to lysine, which retains the ability to form a single ionic interaction, and to glutamine which completely removes the basic side chain (Table 2). Although R96 mutations reduce affinity for **1** (e.g., 63-fold for R96K), these mutants are less stable than sc11F8 (Table 3). R96 is first residue of HCDR3 and is located at the base of the hypervariable region. Residues at the ends of HCDR3 can be buried and not involved in direct ligand interactions (*66*, *67*). Disruption of hydrogen bonding patterns at the base of CDRs can dramatically change the conformation of the binding site, resulting in changes in affinity and specificity (*68*, *69*). The data for R96 mutants suggest that this residue may be more important in maintaining the structure of the binding site, rather than interacting with DNA.

Table 1: Thermodynamic Parameters for 11F8 F(ab) and Sc11F8 Binding to **1**[a]

11F8 Ab fragment	ΔG°_{obs} (kcal·mol^{-1})	ΔC_p (kcal mol^{-1} K^{-1})	ΔH°_{obs} (kcal·mol^{-1})	$T\Delta S^\circ_{obs}$ (kcal·mol^{-1})
F(ab)	-10.8 ± 0.2	-1.1 ± 0.2	-18 ± 3	-7 ± 1
sc11F8	-10.9 ± 0.6	-0.8 ± 0.1	-17 ± 2	-6 ± 1

[a] ΔG°_{obs} values were obtained from affinities measured by fluorescence quenching at 25 °C in 20 mM Tris, pH 8, 150 mM NaCl. Enthalpy data were obtained by van't Hoff analysis over the temperature range of 5 to 35 °C in the same buffer. Errors for ΔG°_{obs} are the standard deviations normalized for number of trials (standard error). Errors for ΔC_p and ΔH°_{obs} reflect uncertainty associated with nonlinear least squares regression. The errors in $T\Delta S^\circ_{obs}$ are standard deviations. While it is possible that the His_6 tag on sc11F8 promotes nonspecific DNA binding, we believe it unlikely given how similar the binding properties of the single chain are compared to the parent F(ab).

Mutating R98 to lysine decreases affinity for **1** ca. 2-fold, relative to the wild-type protein, whereas R98Q binding drops 6-fold. These data suggest that the positive charge of R98 is involved in recognition of **1**. In contrast, mutation of R31 to either lysine or glutamine has a much larger effect on binding affinity (10- and 45-fold, respectively; Table 3). These data suggest that R31 contributes more to recognition than R98. $KMnO_4$ and DMS footprinting of these mutants was performed to determine if any of the bases of **1** interact with R31 and R98. DMS is a reagent that alkylates the N7 of guanine, and $KMnO_4$ oxidizes the C5−C6 double bond of single-stranded thymine (cytosines at the stem-loop junction like dC_{12} in **1** are also susceptible to oxidation which

Table 2: Sc11F8 Mutants[a]

protein	loop location	C_m (M)
sc11F8		1.33 ± 0.11
R31K	HCDR1	0.95 ± 0.23
R31Q		1.12 ± 0.14
$Y32_HF$	HCDR1	1.40 ± 0.12
$Y32_HA$		1.35 ± 0.11
W33F	HCDR1	1.35 ± 0.15
W33V		1.30 ± 0.21
Y56F	HCDR2	1.35 ± 0.14
Y56A		1.28 ± 0.13
R96K	HCDR3	0.52 ± 0.08
L97A	HCDR3	1.51 ± 0.22
R98K	HCDR3	1.28 ± 0.16
R98Q		1.49 ± 0.22
Y99F	HCDR3	1.49 ± 0.11
Y99V		0.37 ± 0.08
Y99A		0.67 ± 0.11
Y100F	HCDR3	1.47 ± 0.21
Y100V		1.10 ± 0.24
$Y32_LF$	LCDR1	1.56 ± 0.21
$Y32_LA$		1.40 ± 0.14

[a] Each residue chosen for mutagenesis was replaced with both a conservative and nonconservative residue. Protein stability was measured in 20 mM Tris, 150 mM NaCl, pH 8 at 25 °C with added guanidine−HCl (0.1−6 M). The concentration of guanidine−HCl at which half the protein is unfolded, C_m, was determined by assuming a linear extrapolation model (*39*). C_m for R96Q mutant could not be determined due to instability of the protein.

Table 3: Relative Affinity of Sc11F8 Mutants for **1**[a]

protein	K_d (**1**) (nM)	relative K_d	ΔG (kcal·mol^{-1})	$\Delta\Delta G$
sc11F8	9.5 ± 0.6	1	−11.0 ± 0.4	0
F(ab)	10.3 ± 0.4	1.1	−10.9 ± 0.3	0.1
R31K	90 ± 9	9.5	−9.6 ± 0.9	1.4
R31Q	410 ± 20	43	−8.7 ± 0.5	2.3
$Y32_HF$	10.9 ± 0.4	1.1	−10.9 ± 0.5	0.1
$Y32_HA$	12.0 ± 0.2	1.3	−10.8 ± 0.3	0.2
W33F	32 ± 1	3.3	−10.2 ± 0.3	0.8
W33V	59 ± 6	6.3	−9.9 ± 0.9	1.1
Y56F	8.8 ± 0.5	0.93	−11.1 ± 0.6	−0.1
Y56A	11 ± 1	1.2	−10.9 ± 0.8	0.1
R96K	590 ± 60	63	−8.5 ± 0.9	2.5
L97A	31 ± 6	3.2	−10.3 ± 0.9	0.7
R98K	16.0 ± 0.7	1.7	−10.6 ± 0.4	0.4
R98Q	58.1 ± 0.8	6.2	−9.9 ± 0.1	1.1
Y99F	9.7 ± 0.8	1.0	−10.9 ± 0.8	0.1
Y99V	121 ± 9	13	−9.4 ± 1.0	1.6
Y100F	5.3 ± 0.3	0.56	−11.3 ± 0.6	−0.3
Y100V	420 ± 50	44	−8.7 ± 0.9	2.3
$Y32_LF$	3.4 ± 0.3	0.36	−11.6 ± 0.9	−0.6
$Y32_LA$	46 ± 6	4.9	−10.0 ± 0.8	1.0

[a] Binding affinity was measured in 20 mM Tris, 150 mM NaCl, pH 8 at 25 °C. Relative K_d values are normalized against K_d for sc11F8. Errors in K_d are the standard error based on a minimum of three trials.

demonstrates that to some extent, they are single stranded; *16*, *70*, *71*). In the presence of wild-type 11F8, T_{10}, T_{11}, dC_{12}, and dG_7 are protected from modification by these reagents (see Figure 2A). Footprinting of R31K and R31Q complexes with **1** shows moderately decreased protection of T_{10} and T_{11} and significantly decreased protection of dG_7 and dC_{12} (Figure 2B). These data suggest that R31 may make specific contacts to dG_7−dC_{12} on **1**. In contrast, the R98 mutants show the same pattern and degree of protection as the wild type, suggesting that this does not participate in base-specific contacts to DNA.

To determine if R31 and/or R98 mediate the cation release that occurs upon binding, affinity measurements as a function of buffer salt concentration were conducted (Table 4). The salt stoichiometry values for R98K, R31K, and the wild-type protein in NaCl and NaOAc are the same, which indicates mutation to lysine does not effect cation or anion release. However, the salt release stoichiometries that characterize binding by R31Q and R98Q are smaller than the values measured for the wild type. Specifically, one less cation is released upon removing the positively charged side chains for both R31 and R98. To determine if R31 and R98 account for the two salt bridges previously proposed for 11F8·**1** complex, the double glutamine mutant (R31Q/R98Q) was studied. Affinity measurements as a function of buffer salt concentration for R31Q/R98Q indicate that the salt stoichiometry values for the double mutant are lower than the single mutants in both NaCl and NaOAc (Table 4). Notably, the affinity of the double mutant for **1** does not change as a function of [NaOAc], indicating that binding of R31Q/R98Q is not accompanied by cation release. In addition, the percentage of binding energy attributable to electrostatic interactions is less than 2% for R31Q/R98Q (vs ca. 23% for sc11F8; see eq 1). These data suggest that R31 and R98 form ionic contacts to the phosphate backbone of **1** and that these residues account for the two salt bridges. Importantly, the decrease in affinity observed for R31K compared to the wild-type protein suggests that R31 is also involved in additional (base-specific) ligand interactions.

Table 4: Salt Release Stoichiometries for Binding of Sc11F8 and Mutants to **1**[a]

protein	salt	$-SK_{obs}$
sc11F8	NaCl	2.3 ± 0.2
	NaOAc	1.5 ± 0.1
R31K	NaCl	2.3 ± 0.1
	NaOAc	1.7 ± 0.2
R31Q	NaCl	1.4 ± 0.1
	NaOAc	1.0 ± 0.1
R98K	NaCl	2.2 ± 0.1
	NaOAc	1.4 ± 0.2
R98Q	NaCl	1.4 ± 0.1
	NaOAc	0.6 ± 0.1
R31Q/R98Q	NaCl	0.86 ± 0.07
	NaOAc	0.14 ± 0.03

[a] Affinity measurements were conducted in Tris buffer (20 mM Tris, 85−300 mM NaCl, pH 8, 25 °C). Values of $-SK_{obs}$ represent the stoichiometry of salt release as described by Record (*42*) and were obtained from the slope of plots of ln K_{obs} vs ln [NaCl]. Errors in $-SK_{obs}$ are the standard deviations associated with slope of the salt plots from thre separate determinations.

Relative Affinity of Mutant Proteins: *Hydrophobic Residues*. Aromatic amino acids often play a role in stabilizing both protein·nucleic acid and anti-DNA·DNA complexes, through base stacking and/or hydrogen bonding (*1*, *13*, *14*). Therefore, Y32 in LCDR1 ($Y32_L$), Y32 ($Y32_H$) and W33 in HCDR1, Y56 in HCDR2, and Y99 and Y100 in HCDR3 were each mutated to phenylalanine and to either alanine or valine (if the alanine mutant was destabilizing) to determine if they participate in ligand recognition (Table 2). Mutation of $Y32_H$ and Y56 to either phenylalanine or alanine does not affect binding, suggesting that these residues are not involved in recognition. While affinity of Y99F for **1** is identical to that for wild-type sc11F8, the affinities of Y99V and Y99A are decreased. However, the stability of these two mutants is also decreased relative to that of the wild type, presumably due to the formation of a destabilizing cavity

(*72*−*74*). Taken together, these data indicate that the aromatic group of Y99 contributes to the stability of the binding cleft. Thus, mutants of $Y32_H$, Y56, and Y99 were not characterized further.

Mutation of either W33 or $Y32_L$ to phenylalanine decreases affinity <3-fold, while W33V and $Y32_L$A bind **1** ca. 6-fold weaker, relative to sc11F8 (Table 3). Footprints of W33V and $Y32_L$A complexed with **1** show that protection of T_{10} and T_{11} is somewhat decreased compared to that of the wild type (Figure 2C). Collectively, these findings suggest that the aromatic side chains of W33 and $Y32_L$ make modest contributions to binding. Substituting Y100 with phenylalanine does not alter affinity for **1**, whereas Y100V binds 44-fold weaker compared to that for the wild type. This large decrease may result from unfavorable steric interactions introduced by the valine side chain. However, the stability of Y100V is similar to that of wild-type sc11F8, which suggests that the drop in affinity results from the loss of a highly complementary recognition surface. This conclusion is also supported by footprinting experiments of Y100V·**1** showing significantly decreased protection of T_{10} and T_{11}, relative to that of the wild-type complex (Figure 2D). Last, changing L97 in HCDR3 to alanine decreases the affinity of **1** 3-fold, relative to the wild type (Table 3). In addition, footprinting experiments of the L97A·**1** complex shows decreased protection of T_{10} and T_{11}, relative to that of sc11F8·**1**, suggesting that L97 may contribute to binding through recognition of these loop nucleotides (Figure 2D).

Relative Affinity of Double Mutant Proteins. Interpretation of results from single residue site-directed mutagenesis experiments assumes that the effects of substitution are localized to the mutated residue (*75*). However, a decrease in binding affinity upon mutation may result from loss of intramolecular interactions with adjacent protein residues, rather than from loss of intermolecular interactions with ligand (*76*). A useful way to probe for such intramolecular interactions is to determine how mutations of two different residues interact with each other in a double mutant protein (*77*−*80*). If the change in free energy associated with a structural or functional property of a protein upon double mutation differs from the sum of changes for the single mutants, then the residues at these two positions must be cooperative and are coupled through either direct or indirect interactions (*77*, *80*). Noncooperativity exists, however, when the effect of the double mutation is equal to the sum of the effects of the single mutations (*81*).

Affinity data for the double mutants binding to **1** were analyzed using double mutant cycles to investigate cooperativity between contact residues. The change in free energy for wild-type sc11F8, single mutants, and the corresponding double mutants binding to **1** is presented in Table 5. These data reveal that very little cooperativity (<0.6 kcal·mol^{-1}) exists between residues of 11F8 and suggest that interactions between residues in the CDRs do not contribute significantly to binding (*82*). Therefore, the decreases in binding energy observed for each single mutant are additive and can be attributed to loss of contacts in the 11F8·**1** complex. Within the limitations of this analysis, residues R31, W33, L97, R98, Y100, and $Y32_L$ account for approximately 80% of the free energy in the 11F8·**1** complex.

Nonspecific Binding. Sequence specificity is often assessed using two criteria (*32*). First, the affinity for a consensus sequence is compared to nonspecific and noncognate ligands (i.e., bulk DNA and sequences that contain elements of the recognition site, respectively). In general, the affinity for a consensus sequence over a nonspecific ligand is >100-fold, and the difference in affinity for a consensus sequence compared to a noncognate ligand often is ≥2-fold. A second criterion to judge sequence specificity employs footprinting experiments. In footprinting experiments, specific complexes are characterized by unique patterns of protection and modification in the recognition site. By contrast, in footprinting nonspecific complexes, unique patterns of protection, and modification are not observed. Using established criteria (*32*), 11F8 is sequence-specific (*16*, *31*).

Table 5: Stability and Cooperativity of Sc11F8 Double Mutants[a]

protein	C_m (M)	$\Delta\Delta G_{DM}$ (kcal·mol^{-1})	$\Delta\Delta G_{SM}$ (kcal·mol^{-1})	ΔG_i (kcal·mol^{-1})
sc11F8	1.40 ± 0.21			
R31Q/W33V	1.73 ± 0.22	1.66	1.65	−0.01
R31Q/L97A	1.60 ± 0.16	1.75	1.72	−0.03
R31Q/R98Q	1.21 ± 0.21	2.36	2.74	0.38
R31Q/Y100V	1.33 ± 0.16	2.39	2.95	0.56
R31Q/$Y32_L$A	1.54 ± 0.17	2.10	1.71	−0.39
W33F/Y100F	1.31 ± 0.18	0.56	0.69	0.12
W33V/$Y32_L$A	1.42 ± 0.15	0.41	0.34	−0.07
L97A/$Y32_L$A	1.41 ± 0.11	0.35	0.43	0.08

[a] Protein stability for each double mutant was measured in 20 mM Tris, 150 mM NaCl, pH 8 at 25 °C with added guanidine−HCl (0.1−6 M). Binding affinity was measured in 20 mM Tris, 150 mM NaCl, pH 8 at 5 °C. $\Delta\Delta G_{DM}$ is the free energy difference between the wild-type sc11F8 and the double mutant binding to **1**. $\Delta\Delta G_{SM}$ is the sum of the free energy difference for each of the single mutants binding to **1**. $\Delta G_i = \Delta\Delta G_{SM} - \Delta\Delta G_{DM}$ and represents the free energy of coupling between the two residues in wild-type sc11F8. Due to the contributions from weak interactions and errors associated with experimental limitations, coupling free energies below ca. 1 kcal·mol^{-1} are generally considered additive (*78*, *115*, *116*).

To investigate how mutation of contact residues within the CDRs of the sc11F8 alters binding specificity, the affinity for a nonspecific ligand, 5′$(GATC)_{13}$GAT (designated **NS**), was investigated (Figure 1 and Table 6). This sequence represents all bases equally and does not possess any secondary structure. Previous experiments have shown that 11F8 IgG binds **NS** >100-fold more weakly than **1**. Recognition is entropy-driven mediated by the release of cations from the DNA phosphate backbone (i.e., polyelectrolyte effect) and is not accompanied by an enthalpy change (*16*).

Mutations to hydrophobic amino acids (W33, L97, Y100, and $Y32_L$) do not alter the affinity for **NS**, relative to the sc11F8·**NS** complex, which is consistent with data showing that recognition of **NS** involving electrostatic interactions with the phosphate backbone. While wild-type sc11F8 binds **1** 125-fold more tightly than **NS**, the affinity of both R31K and R31Q are within ca. 10-fold of their respective affinity for **1**. Hence, these mutants are less sequence-specific than the wild-type protein. This reduced specificity is due to reduced affinity for **1**; i.e., mutation to R31 has a greater affect on sequence-specific binding relative to nonspecific recognition. In contrast, mutation of R98 to lysine does not alter recognition of **1** and **NS**, relative to sc11F8. However, the affinity of R98Q for **1** and **NS** is decreased 9- and 2-fold, respectively, relative to that of the wild type. These data suggest that R98 contributes to both sequence-specific and nonspecific recognition through similar interactions with the phosphate backbone.

Table 6: Affinity of Sc11F8 and Mutants for **1** and **NS**[a]

protein	loop designation	K_d (**1**) (nM)	relative K_d	K_d (**NS**) (nM)	relative K_d	K_d (**NS**)/K_d (**1**)
sc11F8		3.5 ± 0.1	1	442 ± 6	1	126 ± 2
R31K	HCDR1	34.4 ± 0.2	9.9	348 ± 49	0.8	10 ± 2
R31Q		250 ± 20	71	730 ± 150	1.7	2.9 ± 0.8
W33F	HCDR1	10.5 ± 0.9	3.0	364 ± 13	0.8	35 ± 3
W33V		24 ± 3	6.8	435 ± 36	1.0	18 ± 3
L97A	HCDR3	10.9 ± 0.9	3.1	487 ± 38	1.1	45 ± 5
R98K	HCDR3	5.6 ± 1	1.6	608 ± 95	1.4	108 ± 28
R98Q		33 ± 1	9.5	831 ± 28	1.9	25 ± 1
Y100F	HCDR3	3.1 ± 0.9	0.9	653 ± 35	1.5	208 ± 13
Y100V		208 ± 21	59	275 ± 82	0.7	1.3 ± 0.4
$Y32_LF$	LCDR1	1.2 ± 0.1	0.3	427 ± 9	1.0	351 ± 22
$Y32_LA$		14.3 ± 0.2	4.1	401 ± 96	0.9	28 ± 6

[a] Due to the reduced affinity of the mutant complexes, binding affinity was measured in 20 mM Tris, pH 8, 100 mM NaCl at 25 °C. Relative K_d values are normalized against K_d for sc11F8. Errors in K_d are the standard error based on a minimum of three independent trials. Since 11F8 occludes about five nucleotides upon binding (*29*), **NS** possesses overlapping binding sites and binding at any given five base long region is equiprobable (*117*). Therefore, fit of the single-site binding isotherm yields apparent K_d values that overestimate the intrinsic single site affinity for this sequence (*44*, *117*).

Table 7: Affinity of Sc11F8 and Mutants for **T7**[a]

protein	loop designation	K_d (**T7**) (nM)	relative K_d	K_d (**T7**)/K_d (**1**)
sc11F8		24.2 ± 2.1	1	6.9 ± 1
R31K	HCDR1	39.1 ± 9.1	1.6	1.1 ± 0.4
R31Q		247 ± 42	10	1.0 ± 0.2
W33F	HCDR1	79 ± 12	3.3	7.5 ± 0.9
W33V		261 ± 79	11	11 ± 4
L97A	HCDR3	83.8 ± 3.7	3.7	7.7 ± 0.9
R98K	HCDR3	35.3 ± 1.2	1.3	6.3 ± 0.9
R98Q		345 ± 13	14	10 ± 1
Y100F	HCDR3	23.6 ± 6.2	0.98	7.5 ± 2
Y100V		240 ± 20	10	1.2 ± 0.1
$Y32_LF$	LCDR1	7.1 ± 1.3	0.3	5.8 ± 0.9
$Y32_LA$		132 ± 6	5.4	9.2 ± 0.9

[a] Due to the reduced affinity of the mutant proteins, binding affinity was measured in 20 mM Tris, 100 mM NaCl, pH 8 at 25 °C. Errors in K_d are the standard error based on a minimum of three trials. Since **T7** contains several different five-base-long binding registers of thymidine, the single-site-binding isotherm yields apparent K_d values that overestimate the intrinsic affinity for **T7** (*117*, *44*).

Noncognate Binding. Similar to other anti-ssDNA and ssDNA-binding proteins, 11F8 displays a base preference for oligo(T), (*29*). Since oligo(T) contains elements of the recognition sequence on **1**, T-rich sequences can be viewed as noncognate ligands (*31*, *32*). Because discrimination between specific and noncognate sequences can have important biological consequences (*32*), the affinity of sc11F8 and mutants for the thymine-rich ligand (**T7**) was examined (Table 7). **T7** replaces nucleotides 3, 8−14, and 16 of **1** with thymine (Figure 1). Analogous to the binding of **1**, 11F8 binding of **T7** is enthalpy-driven and opposed by entropy (*16*).

Since hydrophobic interactions are involved in binding of **T7**, it was anticipated that W33, L97, Y100, and/or $Y32_L$ would be involved in noncognate recognition. Similar to the wild type, W33F, Y100F, and $Y32_LF$ mutants bind **1** ca. 7-fold more tightly than **T7**. Thus, substitution of these amino acid side chains with phenylalanine has a similar affect on both sequence-specific and noncognate binding. W33V, L97A, and $Y32_LA$ each bind **1** ca. 10-fold more tightly than **T7**. This apparent increase in specificity results from a reduced affinity for **T7** (vs an increased affinity for **1**), possibly due to the removal of hydrophobic interactions with thymine bases of **T7**. In contrast, Y100V does not discriminate between **1** and **T7**, which results from a decreased affinity for **1**, indicating that sequence-specific binding is more affected by removal of the aromatic side chain of Y100 than noncognate binding. Together, these data indicate that L97 and the aromatic side chains of W33 and $Y32_L$ are involved in both sequence-specific and noncognate recognition, whereas only Y100 (and R31) contribute to sequence-specific binding of **1**.

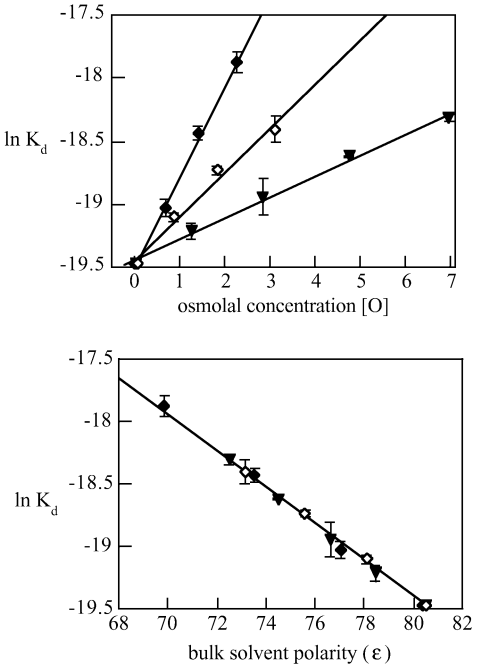

FIGURE 3: Dependence of sc11F8 affinity for **1** on solvent polarity, presented as a function of (A) osmolal concentration and (B) bulk solution dielectric constant. Affinity was measured at 25 °C in 20 mM Tris, 100 mM NaCl, pH 8, in the presence of up to 20% either methanol (▼), ethanol (◇), or 1-propanol (◆). Dielectric constant values represent bulk solution and are thus normalized for polarity differences between individual solvents.

Binding Thermodynamics of Mutant Proteins. Previous experiments have determined that the affinity for **1** decreases as the binding medium becomes less polar. Similar to 11F8 IgG, the dependence of binding affinity of the sc11F8 is independent of the bulk solution polarity but is solvent-dependent with respect to osmolal concentration (Figure 3). These observations suggest that the decreased affinity is primarily due to a reduction in bulk solution polarity, rather

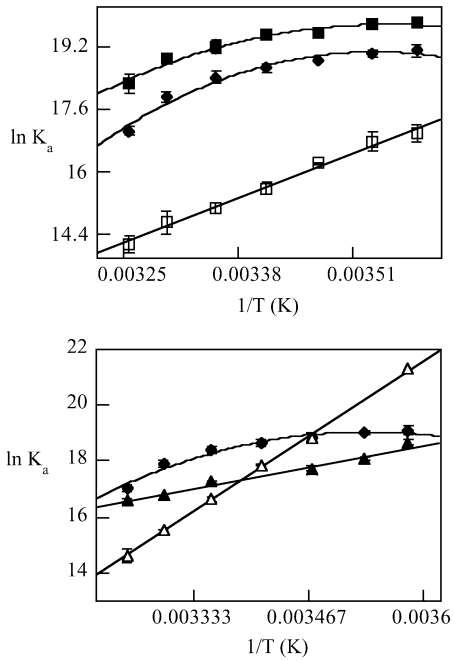

FIGURE 4: van't Hoff analysis of sc11F8 and mutants binding to **1**. (A) sc11F8 (◆), Y100F (■), and Y100V (□). (B) sc11F8 (◆), W33F (▲), and W33V(△). Data were measured in 20 mM Tris, 150 mM NaCl, pH 8, and analyzed assuming a constant negative heat capacity for sc11F8 and Y100F and no change in heat capacity for the other mutants.

than to changes in osmotic stress. Like the parent IgG, it appears that hydrophobic interactions between nonpolar surfaces on the sc11F8 and **1** dominate the favorable enthalpy change associated with binding to **1**. To determine the contribution of individual hydrophobic residues to the overall binding thermodynamics, experiments measuring affinity as a function of temperature and solution polarity were conducted for W33, L97, Y100, and $Y32_L$ mutants.

The van't Hoff plots (ln K_{obs} vs ln 1/T) of $Y32_LF$·**1** and Y100F·**1** are curved, reflecting a negative change in heat capacity change upon binding (Figure 4A) (see Supporting Information). Similar to that observed for sc11F8, the maximum of the van't Hoff plot is near 0 °C, indicating that binding is enthalpically driven throughout the physiological temperature range. In contrast, the van't Hoff plots of W33F, W33V, L97A, Y100V, and $Y32_LA$ are linear, which suggests that binding is not accompanied by a change in heat capacity (Figure 4) (see Supporting Information). The negative heat capacity change reflects a shift in the thermodynamic driving force from entropic at low temperature to enthalpic at higher temperatures and has frequently been interpreted as reflecting the presence of the hydrophobic effect in the recognition process (*40*, *83*). Although other factors can contribute to a $-\Delta C_p$, such as vibrational and conformational entropy accompanying binding, alterations in hydrogen bonding or ion pairing, and any temperature-coupled equilibria, these effects are thought to be less significant contributors than the hydrophobic effect (*40*, *84*). Consequently, the removal of critical binding site residues, particularly those that contribute to the hydrophobic effect, is likely to affect the heat capacity change with binding.

The temperature data for each mutant was fit to an equation that assumes constant heat capacity change (Y100F and $Y32_LF$) or a zero heat capacity change (W33F, W33V, L97A, Y100V and $Y32_LA$), and the resulting enthalpy and entropy values are presented in Table 8. The data indicate that the unfavorable entropy change upon binding is smaller for W33F·**1**, L97A·**1**, Y100F·**1** and $Y32_LF$·**1**, and $Y32_LA$·**1** complexes, relative to that for the wild-type complex. These mutant complexes also have a less favorable enthalpy change that may reflect decreased contacts at the binding interface. In fact, footprinting of L97A·**1** and $Y32_LA$·**1** shows decreased protection of T_{10} and T_{11} compared to that of the wild type, suggesting that the complimentary binding surface has been disrupted (see Figure 2C, D). However, footprints of the phenylalanine-substituted mutants complexed with **1** shows the same pattern and degree of protection as sc11F8, suggesting that Y100F, W33F, and $Y32_LF$ contact similar nucleotides as sc11F8 (see Supporting Information). These data indicate that other factors, such as changes in water structure or the number of polar or hydrophobic interactions, are responsible for the decreased enthalpy change. In contrast, binding of **1** by W33V and Y100V is accompanied by an enthalpy increase, relative to that for sc11F8. Since these mutants bind **1** weaker than the wild type, decreased affinity results from a larger unfavorable entropy change (vide infra).

Table 8: Thermodynamic Parameters Associated with Sc11F8 and Mutants Binding to **1**[a]

protein	ΔC_p (kcal mol^{-1} K^{-1})	ΔH°_{obs} (kcal·mol^{-1})	$-T\Delta S^\circ_{obs}$ (kcal·mol^{-1})
sc11F8	-0.8 ± 0.1	-17 ± 2	6 ± 1
W33F	0	-11 ± 1	1.2 ± 0.1
W33V	0	-38 ± 2	28 ± 1.1
L97A	0	-16 ± 1	5.6 ± 0.2
Y100F	-0.8 ± 0.2	-12 ± 2	0.6 ± 0.1
Y100V	0	-18 ± 1	9.0 ± 0.4
$Y32_LF$	-0.5 ± 0.1	-13 ± 3	1.9 ± 0.4
$Y32_LA$	0	-15 ± 1	5.4 ± 0.4

[a] Enthalpy data were obtained by van't Hoff analysis over the temperature range of 5−35 °C in 20 mM Tris, pH 8, 150 mM NaCl. Errors reported for ΔC_p and ΔH°_{obs} reflect uncertainty associated with nonlinear least squares regression or the standard deviation of the slope of the linear van't Hoff plot. The errors in $T\Delta S^\circ_{obs}$ are standard deviations.

The exclusion of water molecules upon burial of hydrophobic residues (i.e., the hydrophobic effect) at a binding interface provides a significant driving force for antibody·antigen and protein·nucleic acid recognition (*72*, *85*−*89*). The dependence of binding affinity with the addition of nonpolar solvents provides a convenient and sensitive technique for investigating the role of the hydrophobic effect in binding (*90*). To determine the contribution of W33, L97, Y100, and $Y32_L$ side chains to the hydrophobic effect in 11F8·**1** binding, the affinity of these mutants was measured in buffers containing up to 20% methanol, ethanol, and 1-propanol (see Supporting Information).

Similar to the wild type, the dependence of the binding affinity for W33F, Y100F and $Y32_LF$ for **1** as a function of bulk solution polarity are independent of solvent (Figure 5). In addition, the net sensitivity of binding affinity to changes in solution polarity for these mutants, reflected by the slope in the plot of ln K_d versus bulk solution dielectric, is similar to that observed for sc11F8. These results suggest that the hydrophobic effect provides a similar net driving force for these mutants binding to **1** as for sc11F8. The differences in their respective thermodynamic parameters, as compared to

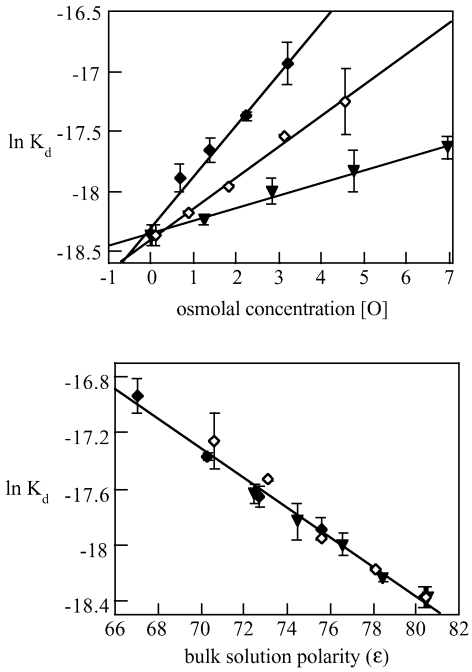

FIGURE 5: Dependence of W33F affinity for **1** on solvent polarity, presented as a function of (A) osmolal concentration and (B) bulk solution dielectric constant. Affinity was measured at 25 °C in 20 mM Tris, 100 mM NaCl, pH 8, in the presence of up to 20% either methanol (▼), ethanol (◇), or 1-propanol (◆). Dielectric constant values represent bulk solution and are thus normalized for polarity differences between individual solvents.

sc11F8 (more favorable entropy and less favorable enthalpy change), may possibly reflect changes to the structure of the water molecules hydrating the 11F8 surface that are introduced by the mutation.

The thermodynamic parameters associated with water release are strongly dependent on the hydration pattern of the hydrophobic surface (*91*). Water release from small, convex surfaces is expected to be entropically favorable due to the highly structured nature of the water molecules in the unbound state (*83*). In contrast, molecular dynamics calculations predict that large planar nonpolar surfaces would be solvated by nonclathrate water structures that are incompletely hydrogen-bonded (*91*). Desolvation of these surfaces is expected to be enthalpically favorable as water molecules become completely hydrogen-bonded in bulk solvent (*91*). In addition, using molecular dynamics simulations, Cheng et al. have demonstrated a strong influence of surface topography on the structure and free energy of hydration over relatively small biomolecular surfaces that contain convex patches, deep or shallow concave grooves and planar areas (*92*).

Southall and Dill have proposed that thermodynamic parameters associated with the hydrophobic effect vary along a continuum ranging from purely entropy-driven with a large negative heat capacity to enthalpy-driven with opposing entropy and no change in heat capacity (*91*). Changes to the surface topography through mutation of residues involved in the hydrophobic effect would be expected to alter the surface topography and hydration pattern and ultimately, the thermodynamic parameters associated with the hydrophobic effect. This phenomenon has been observed for several systems where enthalpy-driven water release provides the primary driving force for binding (*91*, *93*). For example,

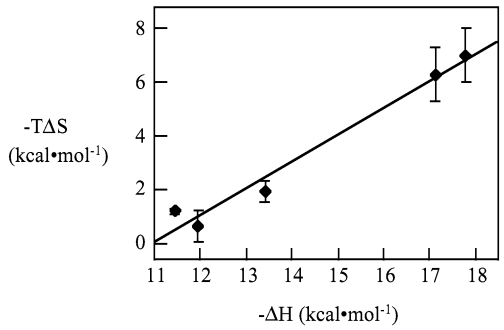

FIGURE 6: Entropy−enthalpy compensation for sc11F8 and mutants binding to **1**. Data included are values obtained for W33F, Y100F, $Y32_LF$, sc11F8, and F(ab) (left to right). The equation of the line is $-T\Delta S = 1.006\ (\Delta H) - 11.02$; $R^2 = 0.986$. Error bars shown are the standard deviation in $-T\Delta S$.

Lemieux et al. found that removal of hydroxyl groups from residues within the protein·carbohydrate recognition surface resulted in small changes to $-\Delta G$ (<1 kcal/mol) but large, compensating changes for values of $-\Delta H$ (more unfavorable) and $-T\Delta S$ (less unfavorable) (*93*). The entropy/enthalpy compensation was attributed to changes in the hydration shell around the positions that were mutated (*93*). Indeed, W33F, Y100F, and $Y32_LF$ of 11F8 show similar enthalpy/entropy compensation (Figure 6). It is possible then that changes in the structuring of water molecules are primarily responsible for the observed shift in thermodynamic parameters for the 11F8 mutants rather than from a loss of interactions at the binding interface for W33F, Y100F, and $Y32_LF$.

The dependence of binding affinity of W33V, L97A, Y100V, and $Y32_LA$ for **1** varies with respect to both bulk solution polarity and osmolal concentration (Figure 7; see Supporting Information). These data suggest that additional factors besides solution polarity are affecting binding of these mutants, such as changes to the enclosed hydrophobic surface area or additional water uptake with binding, that are reflected in the sensitivity of affinity to osmolal concentration (*74*, *94*, *95*).

DISCUSSION

Recognition of ssDNA Involves a Small Number of Residues. Affinity data for the 11F8 double mutants indicate that residues involved in recognition are not significantly coupled. The decrease in binding energy observed for each mutation (where the structural integrity of the protein is retained) can therefore be attributed to a loss of interaction with the **1** and not to indirect effects within the binding surface (*96*). Approximately 80% of the free energy for 11F8 binding to **1** can be ascribed to R31, W33, L97, R98, Y100, and $Y32_L$, while R31 and Y100 alone contribute >40%. Similar observation of a "functional" or "energetic" hotspot have been described for several antibodies, such as HyHEL-10 and D1.3 binding to hen eggwhite lysozyme (*72*, *85*, *97*).

Kinetic data for sequence-specific binding by 11F8 are consistent with a two-step process where the first step involves the formation of an encounter complex, driven by electrostatic steering. In the second step, conformational adjustments occur that promote the energetically favorable exclusion of water molecules to maximize favorable interactions (*15*). Hence, residues responsible for the hydrophobic effect (W33, L97, Y100, and $Y32_L$) may be involved in the

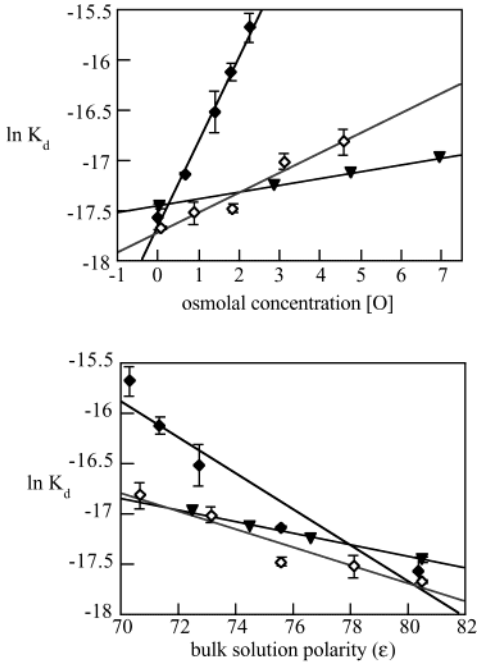

FIGURE 7: Dependence of W33V affinity for **1** on solvent polarity, presented as a function of (A) osmolal concentration and (B) bulk solution dielectric constant. Affinity was measured at 25 °C in 20 mM Tris, 100 mM NaCl, pH 8, in the presence of up to 20% either methanol (▼), ethanol (◇), or 1-propanol (◆). Dielectric constant values represent bulk solution and are thus normalized for polarity differences between individual solvents.

second step of the binding mechanism, whereas R98 and R31 are likely to participate in the formation of the encounter complex. However, data for the R31 mutants indicate that this residue contributes to recognition through additional base-specific contacts and it is not possible to deduce a priori in which step these contacts occur. Although sequence-specific contacts involving arginine has been observed in many protein·nucleic acid systems, the interaction of R31 with **1** is perhaps most similar to the role arginine residues play in some RNA-binding proteins (*98*−*103*). For example, sequence discrimination by the U1A RNA binding protein is achieved through interaction of R52 with the loop closing G−C base pair of its RNA consensus sequence. Binding is thought to occur by the docking of the U1A recognition loop at the RNA stem-loop junction. This interaction may be essential to precisely define the relative position of the double helical stem and single-stranded loop nucleotides, which then make additional contacts for complex stabilization (*99*, *101*, *104*, *105*). It is possible that the sequence-specific recognition of dG_7-dC_{12} by R31 provides a similar role in 11F8 binding to **1**.

Role of Aromatic Residues in the Hydrophobic Effect. The sensitivity of affinity for **1** with buffer polarity for W33F, Y100F, and $Y32_LF$, relative to that of sc11F8, suggests that a comparable amount of hydrophobic surface area is enclosed in the complex for these mutants. The polarity data suggest that the differences in the thermodynamic parameters for these mutants reflect changes to the structure of water molecules hydrating the 11F8 surface that are introduced by the mutation. The affinity and footprinting data for alanine and valine substitutions at these positions indicate that decreased affinity may be due to fewer contacts at the binding interface. Collectively, the data for hydrophobic residues of

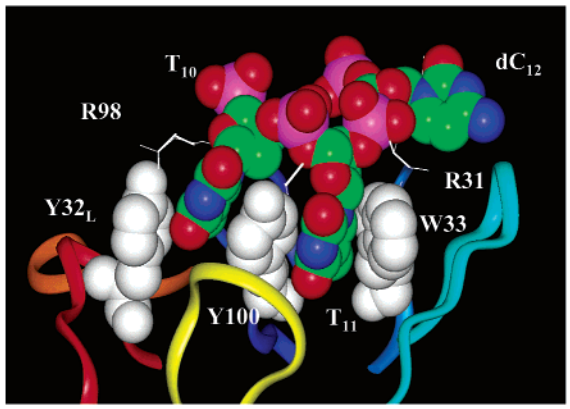

FIGURE 8: Model of $T_{10}-T_{11}-dC_{12}$ of **1** docked into 11F8 binding site. A model of 11F8 was constructed using the methods of Chothia and Lesk (*50*, *118*) as implemented in the INSIGHT software and the general computational approach has been described elsewhere (*119*). The central thymine was docked into the putative binding pocket between ^{Y100}HCDR3 (white) and ^{W33}HCDR1 (white) and oriented such that the C5 methyl group interacts with ^{L97}HCDR3. The second thymine was docked between ^{Y100}HCDR3 and ^{Y32}LCDR1. The cytosine was oriented toward ^{R31}HCDR1. The docked complex was then minimized to a root-mean-square deviation of 0.64 Å. CDRs, shown as ribbons, are colored as followed: HCDR1, medium blue; HCDR2, turquoise; HCDR3, purple; LCDR1, red; LCDR2, orange; LCDR3, yellow.

11F8 (W33, L97, Y100, and $Y32_L$) binding to **1** suggest that these residues contribute to ssDNA binding though interactions with thymine bases and contribute to the favorable enthalpy associated with the hydrophobic effect.

On the basis of the two available crystal structures of anti-DNA complexed with poly(T), Tanner et al. have proposed a "ssDNA-antibody recognition module" for distinguishing between ss- and dsDNA, and perhaps for enforcing sequence specificity (*14*). This module involves the recognition of two consecutive thymine bases, with the majority of contacts to the bases rather than the phosphate backbone. Similar to RNA binding proteins such as U1A, stacking interactions predominate at the interface, with ^{Y32}LCDR1 stacking in parallel above the base and a second aromatic side from HCDR3 stacking below the base (Y100 in DNA-1 and W100a in BV04−01; *13*, *14*). Interestingly, the co-complex of anti-RNA Jel103 complexed with poly (rI) has a similar recognition motif: ^{Y32}LCDR1 stacks above the base, and ^{R96}HCDR3 stacks below the base (*106*). These data suggest that antibodies may use similar strategies for the recognition of single-stranded nucleic acids. Indeed, it appears that 11F8 may bind ssDNA in a similar fashion with stacking interactions provided by ^{Y32}LCDR1 and ^{Y100}HCDR3. However, data from 11F8 mutagenesis experiments extend the model to include additional interactions with W33, hydrophobic contacts from L97, and nonspecific electrostatic interactions from R98 (Figure 8).

Sequence analysis of 11F8 indicates that W33 and $Y32_L$ are germline-encoded. Analysis of previously reported murine and human anti-DNA genes reveals that these residues occur with high frequency (ca. 30% and 96%, respectively) and rarely undergo somatic mutation (*107*). Similarly, approximately 40% of these anti-DNA sequences contain leucine within HCDR3, and ca. 30% of these are located at position 97 (*107*). These data suggest hydrophobic residues may be important for recognition of DNA (*26*, *27*, *108*, *109*) and imply that certain germline residues provide a general

binding surface for recognition of ssDNA and contribute to a (limited) base preference for oligo(T). Our data demonstrate that additional recognition elements are required for sequence-specific discrimination. Hence, the autoimmune response to DNA is similar to the normal immune response (to proteins and haptens) in that critical somatic mutations are required for recognizing antigens with high affinity and specificity (*85*, *110*, *111*).

Unlike aromatic residues, basic residues, particularly arginine, are not common to antibody binding sites (*1*); yet somatic mutations and unusual germline rearrangements, which increase the number of arginine residues in the CDR loop regions, are often present in anti-DNA (*48*). Consistent with this observation, R98 and R31 of 11F8 originate from N-addition and a somatic mutation, respectively, and both of these residues contribute to ssDNA binding. In fact, arginine often plays important and diverse roles in the binding of nucleic acids (*98*−*100*, *102*, *112*, *113*), and it is likely that anti-DNA have incorporated this recognition element specifically for this purpose. Approximately 50% of the reported J558 V_H sub-families encode serine at position 31 of HCDR1, similar to the 11F8 germline sequence (*60*, *107*). Importantly, mutations at this position (ca. 20% of the anti-DNA sequences) suggest a functional role for residues at this site. In support of this hypothesis, mutation of ^{S31}HCDR1 to arginine in anti-DNA mAb 3H9 increased affinity for DNA (*48*).

CONCLUSIONS

Residues that confer sequence specificity to 11F8 are not present in clonally related mAbs, and these other antibodies are neither sequence-specific nor pathogenic. Critical mutations that can confer sequence specificity to anti-DNA may therefore be a feature of pathogenic anti-DNA (*48*, *114*). The ability to identify pathogenic anti-DNA on the basis of primary sequence may ultimately prove useful for diagnostic purposes. The thermodynamic and kinetic basis for specific, noncognate, and nonspecific binding of ssDNA by 11F8 has been determined (*15*, *16*, *31*). Results from mutagenesis studies presented here demonstrate that sequence specificity is predominantly conferred by R31 and Y100. These residues apparently contribute to sequence-specific binding through base-specific hydrogen bonds/electrostatic interactions and base stacking, respectively, and these types of contacts have been observed in a range of protein·nucleic acid systems. In aggregate, however, the interactions and driving forces that mediate recognition of **1** are most closely related to protein·RNA complexes such as those with U1A. Both 11F8 and U1A use elements of β-structure to facilitate binding. This observation suggests that structural similarity at the protein level may be more important than the nucleic acid target (i.e., ssDNA or ssRNA) in determining the optimal interactions to achieve high affinity, specific binding.

SUPPORTING INFORMATION AVAILABLE

Table of the affinity of sc11F8 and mutant; figures of the quantification of $KMnO_4$ and DMS protection and van't Hoff analysis of sc11F8 and mutants. This material is available free of charge via the Internet at http://pubs.acs.org.

REFERENCES

1. Mian, I. S., Bradwell, A. R., and Olson, A. J. (1991) *J. Mol. Biol. 217*, 133−151.
2. Tan, E. M. (1989) *Adv. Immunol. 44*, 93−151.
3. Isenberg, D. A., Ehrenstein, M. R., Longhurst, C., and Kalsi, J. K. (1994) *Arthritis Rheum. 37*, 169−180.
4. Foster, M. H., Cizman, B., and Madaio, M. P. (1993) *Lab. Invest. 69*, 494−507.
5. Ohnishi, K., Ebling, F. M., Mitchell, B., Singh, R. R., Hahn, B. H., and Tsao, B. P. (1994) *Int. Immunol. 6*, 817−830.
6. Voss, E. W. J. (1988) *Anti-DNA Antibodies in SLE*, CRC Press Inc., Boca Raton, FL.
7. Eilat, D., and Anderson, W. F. (1994) *Mol. Immunol. 31*, 1377−1390.
8. Blatt, N. B., and Glick, G. D. (1999) *Pharmacol. Ther. 83*, 125−139.
9. Ballard, D. W., and Voss, E. W. J. (1985) *J. Immunol. 135*, 3372−3380.
10. Isenberg, D. A., Rahman, M. A., Ravirajan, C. T., and Chelliah, T. K. (1997) *Immunol. Today 18*, 149−153.
11. Barry, M. M., Mol, C. D., Anderson, W. F., and Lee, J. S. (1994) *J. Biol. Chem. 269*, 3623−3632.
12. Jang, Y.-J., Sanford, D., Chung, H. Y., Baek, S. Y., and Stollar, B. D. (1998) *Mol. Immunol. 35*, 1207−1217.
13. Herron, J. N., He, X. M., Ballard, D. W., Blier, P. R., Pace, P. E., Bothwell, A. L. M., Voss, E. W. J., and Edmundson, A. B. (1991) *Proteins 11*, 159−175.
14. Tanner, J. J., Komissarov, A. A., and Deutscher, S. L. (2001) *J. Mol. Biol. 314*, 807−822.
15. Beckingham, J. A., and Glick, G. D. (2001) *Bioorg. Med. Chem. 9*, 2243−2252.
16. Ackroyd, P. C., Cleary, J., and Glick, G. D. (2001) *Biochemistry 40*, 2911−2922.
17. Komissarov, A. A., Calcutt, M. J., Marchbank, M. T., Peletskaya, E. N., and Deutscher, S. L. (1996) *J. Biol. Chem. 271*, 12241−12246.
18. Braun, R. P., and Lee, J. C. (1986) *Nucleic Acids Res. 14*, 5049−5065.
19. Rumbley, C. A., Denzin, L. K., Yantz, L. S. Y. T., and Voss, E. W., Jr. (1993) *J. Biol. Chem. 268*, 13667−13674.
20. Smith, R. G., and Voss, E. W., Jr. (1990) *Mol. Immunol. 27*, 463−470.
21. Kubota, T., Akatsuka, T., and Kanai, Y. (1986) *Immunol. Lett. 14*, 53−58.
22. Hermann, M., Winkler, T. H., Fehr, H., and Kalden, J. R. (1995) *Eur. J. Immunol. 25*, 1897−1904.
23. Lee, J. S., Dombroski, D. F., and Mosmann, T. R. (1982) *Biochemistry 21*, 4940−4945.
24. Kneale, G. G. (1992) *Curr. Opin. Struct. Biol. 2*, 124−130.
25. Meyer, R. R., and Laine, P. S. (1990) *Microbiol. Rev. 54*, 342−380.
26. Shamoo, Y., Friedman, A. M., Parsons, M. R., Konigsberg, W. H., and Steitz, T. A. (1995) *Nature 376*, 362−366.
27. Folmer, R. H. A., Nilges, M., Papavoine, C. H. M., Harmsen, B. J. M., Konings, R. N. H., and Hilbers, C. W. (1997) *Biochemistry 36*, 9120−9135.
28. Lopez, M. M., Yutani, K., and Makhatadze, G. I. (1999) *J. Biol. Chem. 274*, 33601−33608.
29. Swanson, P. C., Ackroyd, C., and Glick, G. D. (1996) *Biochemistry 35*, 1624−1633.
30. Swanson, P. C., Yung, R. L., Blatt, N. B., Eagan, M. A., Norris, J. M., Richardson, B. C., Johnson, K. J., and Glick, G. D. (1996) *J. Clin. Invest. 97*, 1748−1760.
31. Stevens, S. Y., and Glick, G. D. (1999) *Biochemistry 38*, 560−568.
32. Jen-Jacobson, L. (1997) *Biopolymers 44*, 153−180.
33. Terada, K., Okuhara, E., Kawarada, Y., and Hirose, S. (1991) *Biochem. Biophys. Res. Commun. 174*, 323−330 and references therein.
34. Laporte, L., Benevides, J. M., and Thomas, G. J. J. (1999) *Biochemistry 38*, 582−588.
35. Bar-Ziv, R., and Libchaber, A. (2001) *Proc. Natl. Acad. Sci. U.S.A. 98*, 9068−9073.
36. Studier, F. W., Rosenberg, A. H., Dunn, J. J., and Dubendorff, J. W. (1990) *Methods Enzymol. 185*, 60.
37. Ho, S. N., Hunt, H. D., Horton, R. M., Pullen, J. K., and Pease, L. R. (1989) *Gene 77*, 51−59.
38. Sarkar, G., and Sommer, S. S. (1990) *BioTechniques 8*, 404−407.
39. Pace, C. N. (1986) *Methods Enzymol. 131*, 266−280.
40. Ha, J.-H., Spolar, R. S., and Record, M. T. J. (1989) *J. Mol. Biol. 209*, 801−816.

41. Baldwin, R. L. (1986) *Proc. Natl. Acad. Sci. U.S.A. 83*, 8069−8072.
42. Record, M. T. J., Lohman, T. M., and deHaseth, P. (1976) *J. Mol. Biol. 107*, 145−158.
43. Record, M. T. J., Anderson, C. F., and Lohman, T. M. (1978) *Quart. Rev. Biophys. 11*, 103−178.
44. Record, M. T. J., and Spolar, R. S. (1990) in *The Biology of Nonspecific DNA-Protein Interactions* (Revzin, A., Ed.) pp 33−69, CRC Press, Boca Raton, FL.
45. Hewitt, G. F. (1970) *Handbook of Chemistry and Physics*, Vol. 51, CRC Press, Boca Raton, FL.
46. Rhodes, D. (1988) in *Protein Function: A Practical Approach* (Creighton, T. E., Ed.) IRL Press, Oxford.
47. Polymenis, M., and Stollar, B. D. (1994) *J. Immunol. 152*, 5318−5329.
48. Radic, M. Z., Mackle, J., Erikson, J., Mol, C., Anderson, W. F., and Weigert, M. (1993) *J. Immunol. 150*, 4966−4977.
49. Jang, Y. J., Lecerf, J.-M., and Stollar, B. D. (1996) *Mol. Immunol. 33*, 197−210.
50. Chothia, C., and Lesk, A. M. (1987) *J. Mol. Biol. 196*, 901−917.
51. Swanson, P. C. (1995) Ph.D. Thesis, University of Michigan, Ann Arbor.
52. Blatt, N. B., Bill, R. M., and Glick, G. D. (1998) *Hybridoma 17*, 33−39.
53. O'Keefe, T. L., Bandyopadhyay, S., Datta, S. K., and Imanishi-Kari, T. (1990) *J. Immunol. 144*, 4275−4283.
54. Tsao, B. P., Ebling, F. M., Roman, C., Panisian-Sahakian, N., Calame, K., and Hahn, B. H. (1990) *J. Clin. Invest. 85*, 530−540.
55. Stewart, A. K., Huang, C., Long, A. A., Stollar, B. D., and Schwartz, R. S. (1992) *Immunol. Rev. 128*, 101−122.
56. Kelley, R. C., Jenson, D. E., and von Hippel, P. H. (1976) *J. Biol. Chem. 251*, 7240−7250.
57. Kim, Y. T., Tabor, S., Churchich, J. E., and Richardson, C. C. (1992) *J. Biol. Chem. 267*, 15032−15040.
58. Collins, K. D., and Washabaugh, M. W. (1985) *Quart. Rev. Biophys. 18*, 323−422.
59. Eilat, D., Webster, D. M., and Rees, A. R. (1988) *J. Immunol. 141*, 1745−1753.
60. Shlomchik, M., Mascelli, H., Shan, H., Radic, M. Z., Pisetsky, D., Rothstein-Marshak, A., and Weigert, M. (1990) *J. Exp. Med. 171*, 265−297.
61. Krishnan, M. R., Jou, N.-T., and Marion, T. N. (1996) *J. Immunol. 157*, 2430−2439.
62. Komissarov, A. A., and Deutscher, S. L. (1999) *Biochemistry 38*, 14061−14067.
63. Bird, R. E., Hardman, K. D., Jacobson, J. W., Johnson, S., Kaufman, B. M., Lee, S. M., Lee, T., Pope, S. H., Riordan, G. S., and Whitlow, M. (1988) *Science 242*, 423−426.
64. Ge, L., Knappik, A., Pack, P., Freund, C., and Pluckthun, A. (1995) in *Antibody Engineering* (Borrebaeck, C. A. K., Ed.) pp 229−266, Oxford University Press, New York.
65. Kuderova, A., Tanha, J., and Lee, J. S. (1994) *J. Biol. Chem. 269*, 32957−32962.
66. Morea, V., Tramontano, A., Rustici, M., Chothia, C., and Lesk, A. M. (1998) *J. Mol. Biol. 275*, 269−274.
67. Satow, Y., Cohen, G., Padlan, E. A., and Davies, D. R. (1986) *J. Mol. Biol. 190*, 593−604.
68. Diamond, B., and Scharff, M. (1984) *Proc. Natl. Acad. Sci. U.S.A. 81*, 5841−5844.
69. Davies, D. R., and Metzger, H. (1983) *Annu. Rev. Immunol. 1*, 87−117.
70. Lustig, B., Bahar, I., and Jernigan, R. L. (1998) *Nucleic Acids Res. 26*, 5212−5217.
71. Long, K. S., and Crothers, D. M. (1999) *Biochemistry 38*, 10059−10069.
72. Braden, B. C., Goldman, E. R., Mariuzza, R. A., and Poljak, R. J. (1998) *Immunol. Reviews 163*, 45−57.
73. Vlassi, M., Cesareni, G., and Kokkinidis, M. (1999) *J. Mol. Biol. 285*, 817−827.
74. Xu, J., Baase, W. A., Baldwin, E. P., and Matthews, B. W. (1998) *Protein Sci. 7*, 158−177.
75. Mildvan, A. S., Weber, D. J., and Kuliopulos, A. (1992) *Arch. Biochem. Biphys. 294*, 327−340.
76. Di Cera, E. (1998) *Adv. Protein Chem. 51*, 59−119.
77. Carter, P. J., Winter, G., Wilkinson, A. J., and Fersht, A. R. (1984) *Cell 38*, 835−840.
78. Wells, J. A. (1990) *Biochemistry 29*, 8509−8517.
79. Ackers, G. K., and Smith, F. R. (1985) *Annu. Rev. Biochem. 54*, 597−629.
80. Horovitz, A. (1996) *Fold Des. 1*, R121−R126.
81. Horovitz, A., Bochkareva, E. S., Yifrach, O., and Girshovich, A. S. (1994) *J. Mol. Biol. 238*, 133−138.
82. Schreiber, G., and Fersht, A. R. (1995) *J. Mol. Biol. 248*, 478−486.
83. Tanford, C. (1980) *The Hydrophobic Effect: Formation of Micelles and Biological Membranes*, John Wiley and Sons, New York.
84. Sturtevant, J. M. (1977) *Proc. Natl. Acad. Sci. U.S.A. 74*, 2236−2240.
85. Dall'Acqua, W., Goldman, E. R., Lin, W., Teng, C., Tsuchiya, D., Li, H., Ysern, X., Braden, B. C., Li, Y., Smith-Gill, S. J., and Mariuzza, R. A. (1998) *Biochemistry 37*, 7981−7991.
86. Kornblatt, J. A., Kornblatt, M. J., Hui Bon Hoa, G., and Mauk, A. G. (1993) *Biophys. J. 65*, 1059−1065.
87. Li, L., and Matthews, K. S. (1997) *Biochemistry 36*, 7003−7011.
88. Sidorova, N. Y., and Rau, D. C. (1996) *Proc. Natl. Acad. Sci. U.S.A. 93*, 12272−12277.
89. Garner, M. M., and Rau, D. C. (1995) *EMBO J. 14*, 1257−1263.
90. Parsegian, V. A., Rand, R. P., and Rau, D. C. (1995) *Methods Enzymol. 259*, 43−94.
91. Southall, N. T., and Dill, K. A. (2000) *J. Phys. Chem. B 104*, 1326−1331.
92. Cheng, Y.-K., and Rossky, P. J. (1998) *Nature 392*, 696−699.
93. Lemieux, R. U. (1996) *Acc. Chem. Res. 29*, 373−380.
94. Pace, C. N. (1992) *J. Mol. Biol. 226*, 29−35.
95. Ysern, X., Fields, B. A., Bhat, T. N., Goldbaum, F. A., Dall'Acqua, W., Schwartz, F. P., Poljak, R. J., and Mariuzza, R. A. (1994) *J. Mol. Biol. 238*, 496−500.
96. Fersht, A. R. (1988) *Biochemistry 27*, 1577−1580.
97. Kelley, R. F., and O'Connell, M. P. (1993) *Biochemistry 32*, 6828−6835.
98. Wilkinson, T. A., Botuyan, M. V., Kaplan, B. E., Rossi, J. J., and Chen, Y. (2000) *J. Mol. Biol. 303*, 515−529.
99. Allain, F. H.-T., Howe, P. W. A., Neuhaus, D., and Varani, G. (1997) *EMBO J. 16*, 5764−5772.
100. Tan, R., and Frankel, A. D. (1993) *Proc. Natl. Acad. Sci. U.S.A. 90*, 1571−1575.
101. Hall, K. B. (1994) *Biochemistry 33*, 10076−10088.
102. GuhaThakurta, D., and Draper, D. E. (2000) *J. Mol. Biol. 295*, 569−580.
103. Calnan, B. J., Tidor, B., Biancalana, S., Hudson, D., and Frankel, A. D. (1991) *Science 252*, 1167−1171.
104. Jessen, T. H., Oubridge, C., Teo, C. H., Pritchard, C., and Nagai, K. (1991) *EMBO J. 10*, 3447−3456.
105. Oubridge, C., Ito, H., Evans, P. R., Teo, C. H., and Nagai, K. (1994) *Nature 372*, 432−438.
106. Pokkuluri, R. P., Bouthillier, F., Li, Y., Kuderova, A., Lee, J. C., and Cygler, M. (1994) *J. Mol. Biol. 243*, 283−297.
107. Radic, M. Z., and Weigert, M. (1994) *Annu. Rev. Immunol. 12*, 487−520.
108. Cusack, S. (1999) *Curr. Opin. Struct. Biol. 9*, 66−73.
109. Draper, D. E. (1999) *J. Mol. Biol. 293*, 255−270.
110. Sharon, J., Gefter, M. L., Manser, T., and Ptashne, M. (1986) *Proc. Natl. Acad. Sci. U.S.A. 83*, 2628.
111. Padlan, E. A. (1994) *Mol. Immunol. 31*, 169−217.
112. Luscombe, N. M., Austin, S. E., Barman, H. M., and Thorton, J. M. (2001) *Genome Biol. 1*, 1−37.
113. Wintjens, R., Lievin, J., Rooman, M., and Buisine, E. (2000) *J. Mol. Biol. 302*, 395−410.
114. Radic, M. Z., Cocca, B. A., and Seal, S. N. (1999) *Crit. Rev. Immunol. 19*, 117−126.
115. Pons, J., Rajpal, A., and Kirsch, J. F. (1999) *Protein Sci. 8*, 958−968.
116. Goldman, E. R., Dall'Acqua, W., Braden, B. C., and Mariuzza, R. A. (1997) *Biochemistry 36*, 49−56.
117. von Hippel, P. H., and Berg, O. G. (1986) *Proc. Natl. Acad. Sci. U.S.A. 83*, 1608−1612.
118. Chothia, C., Lesk, A. M., Levitt, M., Amit, A. G., Mariuzza, R. A., Phillips, S. E. V., and Poljak, R. J. (1986) *Science 233*, 755−758.
119. Eagan, M. A., Norris, J. M., Cooper, B. C., and Glick, G. D. (1995) *Bioorg. Chem. 23*, 482−498.

BI0203942